ELSEVIER

International Journal of Mass Spectrometry 201 (2000) 23–40

International Journal of Mass Spectrometry

Collisional activation, neutralisation–reionisation, and computational studies of $[Ge,C,H_n]^{0/+}$, $n = 2,3$

Phillip Jackson, Ragampetra Srinivas, Norbert Langermann, Martin Diefenbach, Detlef Schröder, Helmut Schwarz*

Institut für Organische Chemie (Sekr. C4), Technische Universität Berlin, Straße des 17, Juni 135, D-10623 Berlin, Germany

Received 13 September 1999; accepted 4 October 1999

Abstract

The ions $[Ge,C,H_2]^+$ and $[Ge,C,H_3]^+$, synthesised using both chemical ionisation (CI) and electron ionisation (EI), have been examined using collisional activation (CA) and neutralisation–reionisation (NR) mass spectrometry. For any method of synthesis, the connectivities Ge-CH_n^+ ($n = 2$–3) are prevalent. NR experiments establish that transitions to the neutral surface from the cation surface, and vice versa, are survived by a large fraction of $[Ge,C,H_2]^+$, and by a much smaller fraction of $[Ge,C,H_3]^+$ parent ions. The modeling of selected points on the surfaces of $[Ge,C,H_2]^{+/0}$ reveals there is little prospect of synthesising neutral or cationic germaacetylene or germavinylidene in sufficient amounts for spectroscopic detection. A general result for all ions and neutrals is that isomer stabilities increase with an increasing number of C–H bonds, in good agreement with available thermochemical data for Ge–H versus C–H bond strengths and previous experimental results for the analogous Si systems. (Int J Mass Spectrom 201 (2000) 23–40) © 2000 Elsevier Science B.V.

Keywords: Organogermanium ions; Mass spectrometry; Ab initio calculations

1. Introduction

Small, fundamental organometallic molecules and ions of germanium can provide insights into gas-phase as well as gas-solid interface processes. For instance, species detected in the low pressure environment of the mass spectrometer could be implicated in the chemical vapour deposition of thin films or be short-lived intermediates in condensed phase chemical reactions that have evaded detection using conventional spectroscopic techniques. It is for these very reasons that ion-beam and ion-trap mass spectrometry will continue to be tools of great importance to chemists at the forefront of material sciences and nanostructure engineering.

Concerning germanium, it is sobering to consult the NIST database 19A [1] to find that heats of formation are available only for the following molecules and ions: $Ge^{-/0/+}$, $GeX^{0/+}$, X = O, S, Ge, Si, and C; $GeH_3F^{0/+}$, $GeX_2H_2^{0/+}$, X = F, Cl, Br, and I; $GeX_4^{0/+}$, X = H, F, Cl, I, and CH_3. Judging by the number of recent publications in this area, this situation is expected to change dramatically over the next few years. Another aspect of research that may indirectly contribute to the burgeoning thermochemical database for Ge-containing species is the search

* Corresponding author. E-mail: Schw0531@www.chem.tu-berlin.de

PII S1387-3806(00)00156-1

for the first example of a Ge-heteroatom triple bond. An example has recently been reported for the lighter congener Si [2].

As an extension of our previous investigation of $[Ge,C,H]^+$ [3], the species $[Ge,C,H_n]^+$, $n = 2–3$, have also been interrogated using the techniques of neutralisation–reionisation (NR) and collisional activation (CA) mass spectrometry. The manifold importance of these studies includes establishing the viability of the corresponding neutrals, determination of the structure of the corresponding ions, and the effects of stepwise reduction and reoxidation on geometric structures. It would also be appealing to confirm the existence of isomeric $[Ge,C,H_n]^+$ ($n = 2–3$) possessing Ge–H bonds, and it is useful to recount the results for the analogous Si systems in this regard. Theoretical studies by Schaefer and co-workers [4], Hopkinson and Lien [5], and Frenking and Stegman [6] suggest that the barriers for the 1,2-H shift for transitions from silavinylidene (H_2SiC) to silaacetylene (HSiCH), and from silaacetylene (HSiCH) to silylidene ($SiCH_2$), are small, and the second of these studies even questions the existence of a silavinylidene minimum. The MS studies of Schwarz and co-workers have confirmed that the neutrals $SiCH_n$, $n = 1–3$, [7] are stable on the microsecond timescale and are accessible from the ions with the same connectivity. Independent theoretical investigations have established that the hydrogen atoms prefer to reside on the carbon atoms [4–8]. There is also one report of an ion–molecule reaction product $CSiH^+$, generated from SiH_n^+ and CO, that is proposed to be a proton source for CO in plasmas [9]. Investigations of the SiH_4/CO system recently conducted in our laboratory using CAMS and NRMS indicate that only ions with Si–C–H connectivity are accessible from this mixture [10,11].

The recently published high resolution absorption spectrum of germylidene [12] and complementary theoretical study [13] captured our interest, particularly because the matrix method is often useful for the isolation and detection of geometric isomers. Although the existence of neutral germylidene ($GeCH_2$) has been unequivocally established, there remains no firm experimental evidence for the existence of either germaacetylene (HGeCH) or germavinylidene (H_2GeC).

Our theoretical study of the systems $[Ge,C,H_n]^+$ employs the semiempirical hybrid density functional theory (DFT) method (B3LYP) proposed by Becke [14,15], which can provide thermochemical information of reasonable accuracy at only a modest computational cost. In this study, we have used a triple-zeta all-electron basis set, augmented with polarisation and diffuse functions for each element, to model the stationary points on the respective cation hypersurfaces. The results obtained from the calculations are complementary to the experimental results, and assist in unraveling the processes occurring in the gas phase.

2. Experimental and computational details

The details of the CAMS and NRMS experimental techniques are comprehensively described in the review articles that have appeared over the last few years [16], so only rudimentary points pertaining to the $GeCH_n^{0/+}$ experiments are presented below. The precursor ions were generated using two different approaches. The first approach involved electron ionisation (EI) of Cl_3GeCH_3 vapour (Gelest Inc.) at pressures of $\sim 10^{-5}$ mbar. This method was successfully used to generate $GeCH^+$ in previous experiments [3]. The second approach involved gas-phase synthesis from GeH_4 (Praxair) and c-C_3H_6 (Linde) in a chemical ionisation (CI) source, with the condition $p(GeH_4) \leq p(c\text{-}C_3H_6)$ favouring the formation of the ions of interest. The gas-phase synthesis of $GeC_mH_n^+$ from Ge^+ and c-C_3H_6 in an ion cyclotron resonance (ICR) cell has recently been reported [17], and species with this stoichiometry have also been observed as the condensation products of $(CH_3)_2GeH_2$ in high pressure MS experiments [18–20]. The chemical ionisation approach involving GeH_4 holds the greatest prospects for synthesising isomers possessing Ge–H bonds if the interconversion barriers connecting $GeCH_n^+$ are sufficiently high. For example, variations in the abundances of GeH_n^+ fragments should be apparent in the CA and NR experiments. In order to ascertain interferences from isobaric species, several

isotopomers corresponding to $[Ge,C,H_2]^+$ and $[Ge,C,H_3]^+$ were selected for analysis. Contaminants, and the methods used to establish their percentage contributions to fragment peaks, are discussed in the relevant results sections.

The experiments were performed using a four-sector modified HF-ZAB AMD 604 mass spectrometer with BEBE configuration, where B and E represent magnetic and electric sectors, respectively. Typical electron ionisation source conditions are as follows: source temperature 200 °C; trap current 100 μA; repeller voltage 15 V; ion extraction voltage 8 kV; $m/\Delta m \geq 1500$. Collisional activation of B(1)E(1)-mass selected $GeCH_n^+$ was effected in collision cells and positioned between E(1) and B(2) using He as a target gas. The collision cell pressure was maintained such that 80% transmittance (T) of the parent ion beam was achieved after passing through this cell. This corresponds to 1.1–1.2 collisions per ion [21,22]. CA products were recorded by scanning the second magnetic sector B(2). NRMS experiments were performed for B(1)E(1)-mass selected $GeCH_n^+$, utilising the dual collision cells between E(1) and B(2). Cation neutralisation was achieved by collision with Xe at 80% T, whereas reionisation was achieved by collision of the neutrals with O_2, again at 80% T. Any cations remaining after the first collision event were deflected from the primary neutral beam using an electrode maintained at a high potential (2 kV) positioned before the second collision cell. In order to detect a recovery signal, the neutral species must be stable for $\sim$1 μs. NRMS spectra were averaged over 40–100 acquisitions in order to obtain sufficient S/N ratios, whereas CA spectra were averaged over 20–50 acquisitions.

B3LYP calculations were performed using GAUSSIAN 94 software [23] on an IBM RS/6000 cluster running AIX 4.2.1. Both doublet and quartet spin states of the cations Ge^+-CH_2, HGe^+-CH, H_2Ge^+-C, and singlet and triplet states of the cations Ge^+-CH_3, H-Ge^+-CH_2 were investigated, and any stationary points were characterised as either minima or transition structures by inspection of the eigenvalues of the hessian matrices. The all-electron triple-zeta basis sets of Krishnan and co-workers (C,H) [24] and McGrath and co-workers (Ge) [25–27] were used throughout. The basis sets were supplemented with single *s* and *p* functions for Ge and H, and single *p* and *d* functions for C. In addition to the cation surfaces, the complete $^1[Ge,C,H_2]^0$ surface was mapped for comparison with previously published coupled-cluster results [13]. To simplify the discussion of the various possible geometric isomers of $[Ge,C,H_n]$, we have adopted the labels **1–6** with reference to Scheme 1. The isomer multiplicity and charge are specified by the leading and trailing superscripts, respectively. For example, $^2\mathbf{1}^+$ refers to a doublet germylidene cation.

3. Results and discussion

Because an accurate interpretation of the experimental results cannot, in many cases, be achieved without an appreciation of the potential-energy surfaces of the respective neutrals and cations, we first present the experimental results. The theoretical results are presented in Sec. 3.3, in which we also elaborate on our initial interpretations.

3.1. $[Ge,C,H_2]^+$

3.1.1. Collisional activation mass spectrometry (CAMS)

The ions at $m/z = 84$, corresponding to $[^{70}Ge,C,H_2]^+$ plus a small amount of $^{72}GeC^+$, as synthesised in the El source from Cl_3GeCH_3, were mass selected for CA analysis [Fig. 1(a)]. Thus, the origin of any ion signal at $m/z = 72$ in the resulting CA spectrum cannot be unambiguously established. For comparative purposes $m/z = 90$ was also analysed because this peak is predominantly $[^{76}Ge,C,H_2]^+$ plus some $^{74}GeO^+$ [Fig. 1(b)]. Formation of $[^{74}Ge,C,H_4]^+$ from Cl_3GeCH_3 in the EI source is highly improbable because ion–molecule reaction conditions are not maintained. Thus, peaks at $m/z = 77$–78 can be unambiguously assigned to $^{76}GeH_n^+$, $n = 1$–2, generated during the activation of $[^{76}Ge,C,H_2]^+$. Signals due to the oxide are attributed to the hydrolysis of the precursor in either the laboratory, the inlet system, or the ion source.

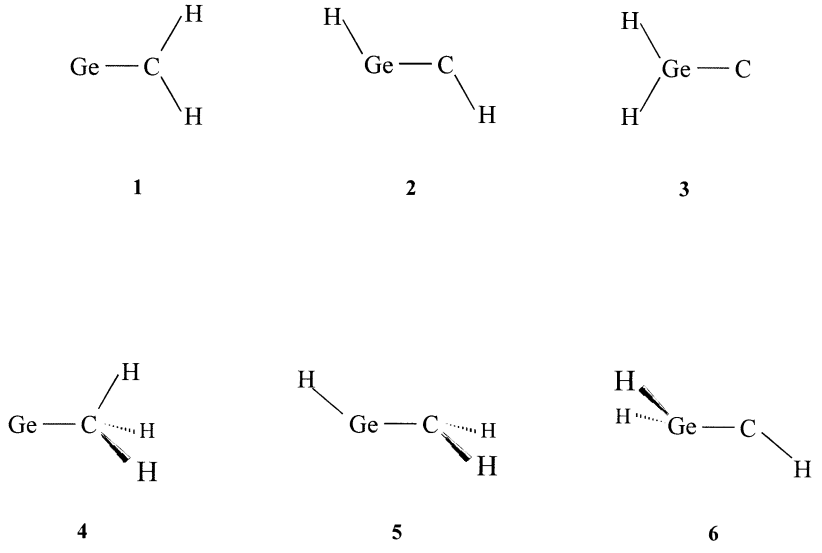

Scheme 1. Structural possibilities for $[Ge,C,H_n]^{+/0}$, $n = 2,3$, studied using theoretical methods. **1** = germylidene; **2** = germaacetylene; **3** = germavinylidene; **4** = methylgermanium; **5** = 1-germavinyl; **6** = 2-germavinyl. Nonplanar structural analogues of 1–3 and planar analogues of **5** are also possible, as are linear **2**.

Inspection of Fig. 1(a) (CA, $m/z = 84$) reveals signals of high intensity corresponding to losses of H ($m/z = 83$) and CH_2 ($m/z = 70$), and minor signals corresponding to losses of 2H ($m/z = 82$), CH ($m/z = 71$) and C ($m/z = 72$). The absence of a peak corresponding to loss of C in the CA spectrum of $m/z = 90$ [Fig. 1(b)] infers that the peak at $m/z = 72$ in Fig. 1(a) might be due entirely to the contaminant $^{72}GeC^+$. Together, the CA spectra presented in Fig. 1(a) and 1(b) suggest $[Ge,C,H_2]^+$ synthesised in the EI source possesses predominantly Ge^+-CH_2 ($\mathbf{1}^+$) connectivity. However, the small but significant GeH_n^+ signals indicate the presence of $\mathbf{2}^+$ or $\mathbf{3}^+$, generated either in the source or by collision-induced isomerisation.

$[^{70}Ge,C,H_2]^+$ was also synthesised in the gas phase by the CI of mixtures of GeH_4 and *c*-C_3H_6. We do not expect, but do not preclude, interference from $^{72}GeC^+$ in the CA spectrum of $m/z = 84$, because bare Ge^+ reacts with *c*-C_3H_6 to form only $GeCH_2^+$ (not GeC^+) [17]. To the best of our knowledge, there is no information available concerning the GeH_n^+/*c*-C_3H_6 couples for $n = 1$–3.

The CA spectrum of $[^{70}Ge,C,H_2]^+$ generated from GeH_4 and *c*-C_3H_6 is presented in Fig. 1(c). Signals of high intensity corresponding to losses of H and CH_2 are evident, whereas signals corresponding to losses of 2H, CH, and C are much weaker. The latter peak is very weak indeed (only 0.8% of the total fragment ion current). In addition, the general features of the CA spectra of EI-synthesised $[^{70}Ge,C,H_2]^+$ appear similar to those generated by CI, with only subtle differences in the peak abundances. This warrants closer scrutiny; of particular importance is any evidence that indicates one approach to be more amenable to the synthesis of $\mathbf{2}^+$.

The normalised abundances of the relevant fragment peaks for the spectra presented in Fig. 1(a)–(c) are given in Table 1. It is immediately apparent that for CI-generated $[Ge,C,H_2]^+$, CH_2 loss is more pronounced than for either of the EI-generated $[Ge,C,H_2]^+$ mixtures. Moreover, the GeH^+/Ge^+ ratio, and the H-loss peaks, are larger for the EI-generated mixtures than for CI-generated $[Ge,C,H_2]^+$. This suggests that a small but significant fraction of EI-generated $[Ge,C,H_2]^+$ exists as isomeric $\mathbf{2}^+$ whereas CI-generated $[Ge,C,H_2]^+$ is predominantly $\mathbf{1}^+$. This latter finding concurs with the results from earlier ICR studies [17], that is, Ge^+ may be the only ion that reacts with *c*-C_3H_6 to yield $[Ge,C,H_2]^+$.

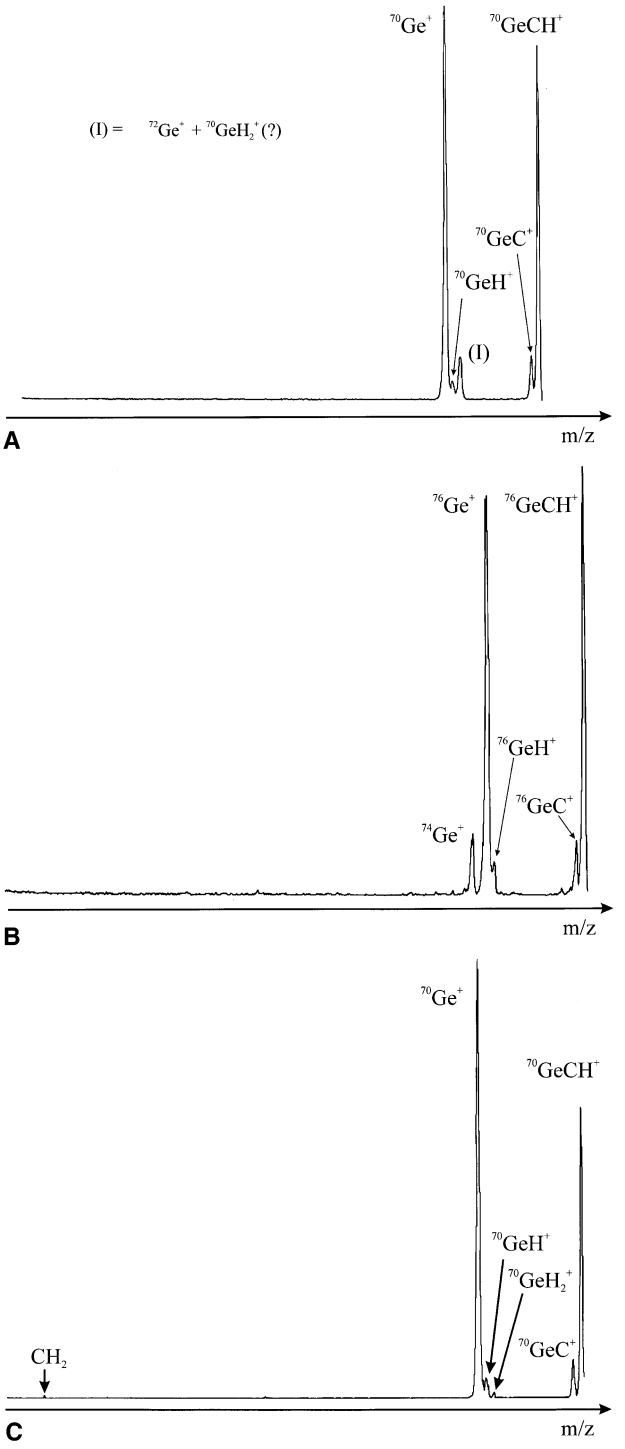

Fig. 1 (a) CA mass spectrum of $m/z = 84$, corresponding to $[^{70}Ge,C,H_2]^+$ and some $^{72}GeC^+$, generated by electron ionisation of Cl_3GeCH_3; (b) CA mass spectrum of $m/z = 90$, corresponding to $[^{76}Ge,C,H_2]^+$ and some $^{74}GeO^+$, generated by electron ionisation of Cl_3GeCH_3; (c) CA mass spectrum of $m/z = 84$, corresponding to $[^{70}Ge,C,H_2]^+$ generated by chemical ionisation of a $GeH_4/c\text{-}C_3H_6$ mixture.

Table 1
Normalised abundances of fragments in the CA spectra of CI- and EI-generated [Ge,C,H_2]. The asterisk denotes that a fraction of this signal corresponds to $^{72}Ge^+$ from CA of $^{72}GeC^+$

	Fragment ions				
Spectrum	Ge^+	GeH^+	GeH_2^+	GeC^+	$GeCH^+$
Fig. 1(a)	0.46	0.02	0.05*	0.05	0.42
Fig. 1(b)	0.44	0.02	0	0.06	0.47
Fig. 1(c)	0.54	0.03	0.01	0.05	0.37

Moreover, the fragmentation signals for both EI- and CI-generated $[GeC,H_2]^+$ indicate a high abundance of $\mathbf{1}^+$. In view of the previous results for the analogous silicon system [7], we conclude that $\mathbf{1}^+$ is the most energetically stable isomer.

3.1.2. Neutralisation–reionisation mass spectrometry (NRMS)

The lack of significant differences in the CA spectra of EI- and CI-generated $[Ge,C,H_2]^+$ suggest that little additional structural information will be gained through NRMS experiments of $[Ge,C,H_2]^+$ synthesised according to both of these approaches. Instead, we have limited our investigations to CI-generated $[^{70}Ge,C,H_2]^+$ because higher yields can be obtained using this method.

A large survivor signal is evident in the NR spectrum of $[^{70}Ge,C,H_2]^+$, as well as a large signal corresponding to loss of CH_2 [Fig. 2(a)]. The other noteworthy features of the spectrum are the low abundances of signals due to $^{70}GeH_n^+$, $n = 1,2$. The remaining high-mass peaks are due to hydrogen losses. The fragmentation pattern is consistent with an ion possessing $\mathbf{1}^+$ connectivity, and the survivor signal implies that **1** is a stable neutral on at least a microsecond timescale. The large signal due to loss of CH_2 suggests that the bond length of **1** is displaced from that of $\mathbf{1}^+$, resulting in significant energy deposition into the neutral molecule formed during vertical electron transfer.

3.2. [Ge,C,H_3]$^+$

3.2.1. CAMS

Unfortunately, there are a great number of isobaric ions that interfere with the CA (as well as NR) analysis of $GeCH_3^+$. For $^{70}GeCH_3^+$ generated by EI of Cl_3GeCH_3, $^{72}GeCH^+$ (germaethynyl) and $^{73}GeC^+$ both contribute to the signal at $m/z = 85$. This leaves $m/z = 91$, $[^{76}Ge,C,H_3]^+$, the least abundant isotopomer, as the only viable signal for analysis. However, interferences are also encountered for this mass, for which hydrolysis of the precursor, either in the source or during sample introduction, produces a small but problematic contribution from $^{74}GeOH^+$. As a result, the first H-loss peak will be attributable to both the ion of interest and the contaminant. In any case, little useful structural information can be derived from the first H-loss peak for species containing more than two hydrogen atoms. For the following reasons, the generation of $\mathbf{4}^+$ from the EI of Cl_3GeCH_3 is anticipated: (1) the precursor already possesses this connectivity, (2) C–H bonds are much stronger than Ge–H bonds, and (3) $\mathbf{4}^+$ can formally be considered a stable, closed shell Ge(II) species. The difference in the strengths of C–H versus Ge–H bonds indicates significant barriers would be associated with hydrogen shifts to form either $\mathbf{5}^+$ or $\mathbf{6}^+$ from $\mathbf{4}^+$, so the EI method of generation, which usually results in the formation of parent ions with high internal energies, may actually work in our favour in this instance. On the other hand, if the potential-energy surface of $[Ge,C,H]^+$ [3] is any guide, reversion will probably be facile.

Interferences from $GeCH_n^+$, $n = 0–2$, are less likely to complicate (to any appreciable extent) the mass spectra of $[^{70}Ge,C,H_3]^+$ synthesised by the CI of GeH_4 and *c*-C_3H_6 mixtures. Given that Ge^+ reacts with *c*-C_3H_6 to form $\mathbf{1}^+$ and C_2H_4, GeH_n^+, $n = 1–3$, might also react to abstract methylene resulting in formation of $\mathbf{5}^+$ or $\mathbf{6}^+$. We believe there is a good chance that the methylene abstraction reaction of the GeH_3^+/*c*-C_3H_6 couple could liberate two neutrals (C_2H_4 and H_2) and leave the product ion, $\mathbf{5}^+$, internally cool. In contrast, ethane might be the exclusive neutral product, in which case a product ion such as $\mathbf{5}^+$ or $\mathbf{6}^+$ might possess the requisite energy to isomerise to $\mathbf{4}^+$. In the following discussion, we will focus on $[^{70}Ge,C,H_3]^+$ generated by the CI of GeH_4/*c*-C_3H_6 mixtures, with some reference to EI-generated $[^{76}Ge,C,H_3]^+$.

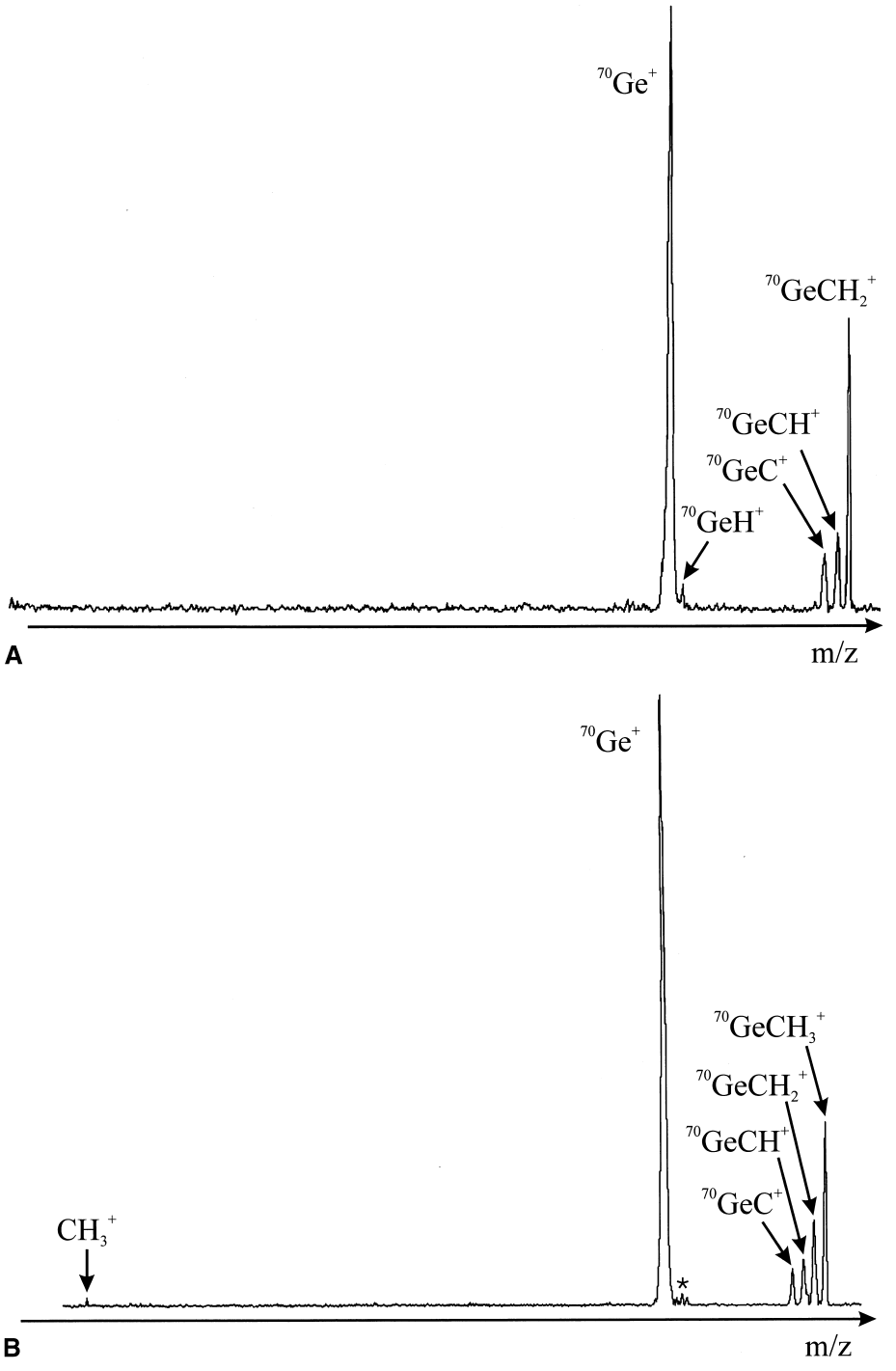

Fig. 2. (a) NR mass spectrum of $m/z = 84$, corresponding to $[^{70}Ge,C,H_2]^+$ generated by chemical ionisation of a $GeH_4/c\text{-}C_3H_6$ mixture; (b) NR mass spectrum of $m/z = 85$, corresponding to $[^{70}Ge,C,H_3]^+$ generated by chemical ionisation of a $GeH_4/c\text{-}C_3H_6$ mixture. The asterisk indicates that these peaks ($m/z = 72$–73) are most likely artefacts arising from discharges in the source. In any case, there is no signal at $m/z = 71$, which casts doubt over the origins of the higher mass signals.

The CA spectrum of CI-generated $[^{70}Ge,C,H_3]^+$ is presented in Fig. 3(a). The base peak in the spectrum corresponds to $^{70}Ge^+$. Typical H-loss peaks are also evident, with monotonically decreasing intensity from $m/z = 84$ to $m/z = 82$. A very small fragment peak corresponding to methyl cation was also detected, but was too weak to be observed in the same spectrum as the base peak. This pattern is entirely consistent with an ion possessing (predominantly) Ge–CH_3 connectivity. The high mass shoulder of the base peak suggests that there are small amounts of $\mathbf{5}^+$ and $\mathbf{6}^+$, formed either in the CI source or by collision-induced isomerisation. Even if a mixture of ions is synthesised by reactions in the CI source, $\mathbf{4}^+$ is by far the most abundant species.

The CA spectrum of EI-generated $[^{76}Ge,C,H_3]^+$ is presented in Fig. 3(b). The broad features of the CA spectrum of CI-generated $[^{70}Ge,C,H_3]^+$ are reproduced in this figure, so there are few points to comment on, other than the peak at $m/z = 74$, which is attributable to $[^{74}Ge,O,H]^+$, as previously discussed. We have independently verified that OH loss is the principal dissociation observed for $[Ge,O,H]^+$ in CA experiments, therefore the contribution of the contaminant ion to the other peaks in the spectrum is negligible.

3.2.2. NRMS

The NR spectrum of CI-generated $[^{70}Ge,C,H_3]^+$ is presented in Fig. 2(b). A survivor ion is evident in the spectrum, as are peaks corresponding to losses of CH_3 (base peak, $m/z = 70$), and 1–3 H atoms ($m/z = 84$ to $m/z = 82$). Note the conspicuous absence of $^{70}GeH_n^+$ ($n = 1$–3) peaks, which suggests that the parent ion is predominantly $\mathbf{4}^+$, and any $\mathbf{5}^+$ that is formed survives $^+NR^+$. There is a very small peak at $m/z = 72$ ($^{70}GeH_2^+$) that might be attributable to $\mathbf{6}^+$ or interferences from $^{72}GeCH^+$. Overall, **4** is a stable neutral on a microsecond timescale, and it will only be a matter of time before **4** is detected in matrix spectroscopic experiments.

The NR spectrum of EI-generated $[^{76}Ge,C,H_3]^+$ (not presented) is also broadly similar to Fig. 2(b), with the notable exception of a smaller survivor ion signal. In this case, the small survivor signal can be rationalised by considering the relative internal energies of the ions produced by CI and EI, with the latter method more likely to produce vibrationally excited (metastable) ions. On the basis of the $^+NR^+$ spectrum of EI-generated $[^{76}Ge,C,H_3]^+$ alone, it would be difficult to conclude that **4** is stable as a neutral because the survivor ion might be entirely due to the interferent $^{74}GeOH^+$.

Now that the MS studies undertaken in this laboratory have established that $GeCH_n^+$, $n = 1$–3, is simple to synthesise in the gas phase and can survive neutralisation from, and reionisation to, the cation surface we ask; why is this connectivity predominantly favoured for all these species, and are the GeH_n^+ ($n = 1$–2) peaks attributable to predissociative isomerisation, or are $HGeCH_n^+$ ($n = 1$–2) isomers also synthesised in the ion source? The density functional theory studies of $[Ge,C,H_n]^+$ ($n = 2$–3) outlined in the following section, should answer these questions.

3.3. Theoretical results

We have limited our theoretical investigations to detailed studies of the $[Ge,C,H_2]^{+/0}$ potential-energy surfaces and the interconversion of $\mathbf{4}^+$ and $\mathbf{5}^+$. Salient features of the singlet $[Ge,C,H_2]$ surface have recently been published [13]. However, upon inspection of the energies and molecular properties reported in this work, we were confronted with a dilemma regarding the relative quality of CCSD/TZDP and CCSD(T)/DZP calculations; that is, which are better and which do we compare with the DFT results? It is difficult to separate the two methods simply on the basis of computational quality, and in the absence of total SCF energies, our choice of CCSD/TZDP is related to inferences in the original report. It is also worthwhile to note that Stogner and Grev [13] have only investigated selected triplet structures on the neutral surface, namely for **1**, whereas we have undertaken more exhaustive studies of the doublet/quartet surfaces of $[Ge,C,H_2]^+$. The results from our studies are presented below, and comparisons are made where it is appropriate.

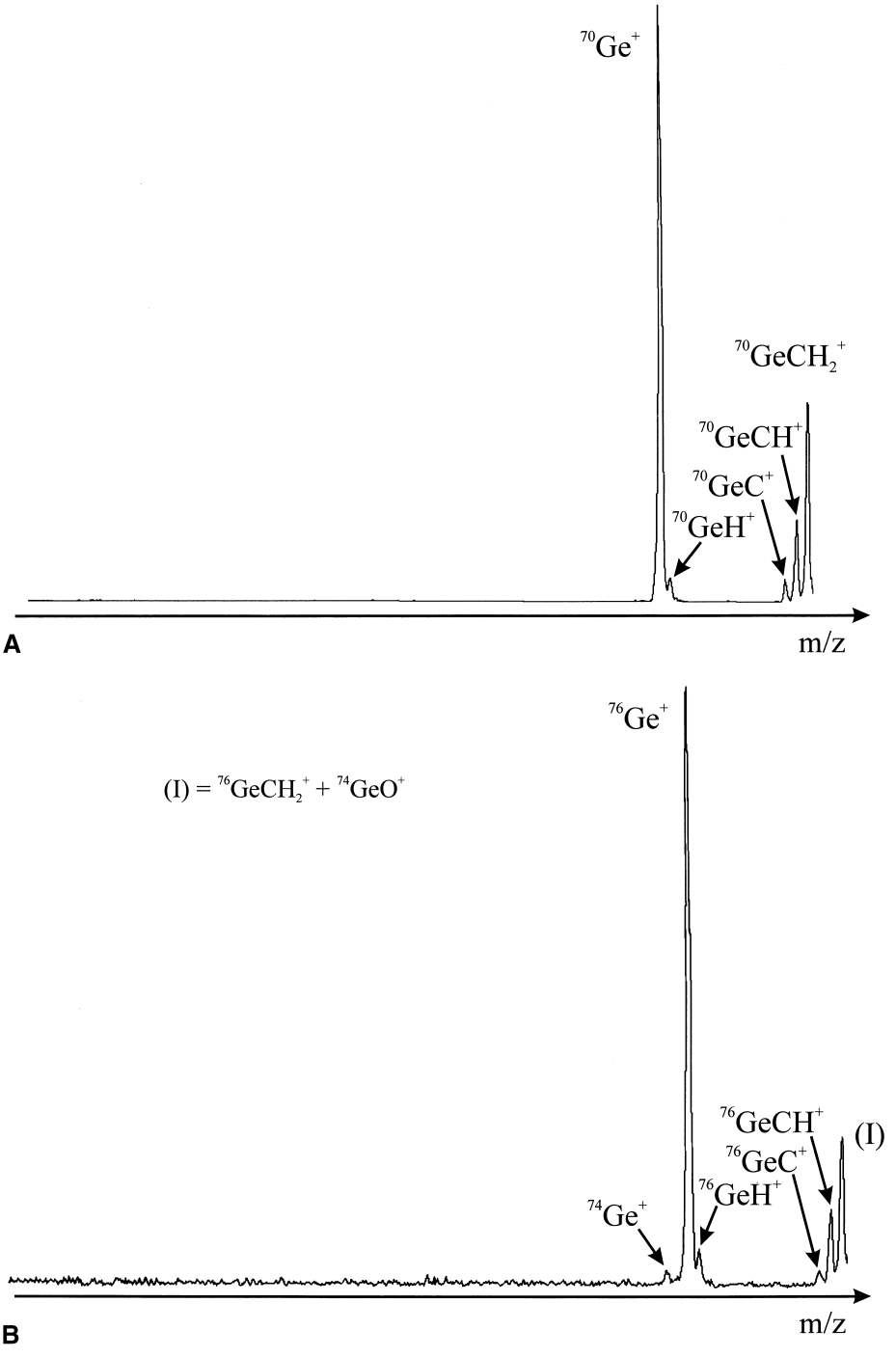

Fig. 3. (a) CA mass spectrum of $m/z = 85$, corresponding to $[^{70}Ge,C,H_3]^+$ generated by chemical ionisation of a $GeH_4/c\text{-}C_3H_6$ mixture; (b) CA mass spectrum of $m/z = 91$, corresponding to $[^{76}Ge,C,H_3]^+$ generated by electron ionisation of Cl_3GeCH_3.

Table 2
Results for the stationary points on the $[Ge,C,H_2]^+$ surfaces located using B3LYP/6-311++G(d,p). SCF energies are in hartrees, bond lengths in Å, zero-point and E_{rel} (ZPE corrected) energies in kcal mol^{-1}. "TS" and "EC" signify saddle point and encounter complex, respectively

Structure	State	E_{SCF}	r_{GeC}	r_{GeH}	r_{CH}	$\theta_{HCH°}$	$\theta_{GeCH°}$	$\theta_{HGeC°}$	E_{rel}	ZPE
^{2}**1**$^+$	$^2B_1$	−2115.9422624	1.914		1.093	113.9	123.0		0.0	13.5
	$^2A_1$	−2115.8852483	1.804		1.090	132.4	113.8		36.4	13.8
	$^2A_2$	−2115.8344099	2.016		1.088	131.6	114.2		68.8	14.0
^{4}**1**$^+$	$^4A_2$	−2115.8461767	2.032		1.087	131.6	114.2		60.7	13.4
	$^4A_1^{TS}$	−2115.8281369	2.277		1.084	140.6	109.7		70.6	11.9
	^4A	−2115.7378060	2.215		1.269, 1.266, 0.955[a]	44.3	125.5		124.3	8.4
^{2}**2**$^+$	$^2\Pi^{TS}$	−2115.8465884	1.693	1.498	1.080		180.0	180.0	58.4	11.3
	$^2\Sigma^{TS}$	−2115.5325040	1.810	1.627	1.154		180.0	180.0	255.4	9.6
	$^2A''$	−2115.8646374	1.823	1.546	1.091		214.6	118.0	46.5	10.9
	$^2A'$	−2115.8321247	1.692	1.495	1.080		174.5	175.4	67.5	11.3
	$^2A''$	−2115.8500827	1.813	1.537	1.090		144.6	119.9	55.7	10.9
^{2}**TS1**	$^2A''^{TS}$	−2115.8602282	1.873	1.600	1.873, 1.094		167.8	82.3	48.3	9.9
	$^2A'^{TS}$	−2115.7886905	1.727	1.611	1.091		159.6	68.6	94.3	10.6
^{4}**2**$^+$	$^4\Pi^{TS}$	−2115.7452480	1.862	1.500	1.084		180.0	180.0	120.7	9.5
EC	$^4\Sigma^{TS}$	−2115.7756281	1.894	3.355	1.090		180.0	180.0	98.9	6.9
	$^4A'^{TS}$	−2115.7482349	1.911	1.507	1.087		211.6	162.5	119.4	10.1
	$^4A''$	−2115.8339783	1.897	1.578	1.092		141.7	119.7	65.9	10.9
^{4}**TS1**	$^4A''^{TS}$	−2115.7624151	1.974	1.771	1.110		240.7	72.7	108.6	8.3
	$^4A''^{TS}$	−2115.7766105	1.911	1.507	1.087		180.0	162.5	100.6	9.3
^{2}**3**$^+$	$^2A_1$	−2115.7368706	1.821	1.514		137.8		111.1	126.2	9.7
	$^2B_1$	−2115.7677260	1.980	1.525		120.9		119.5	106.2	9.2
EC	$^2B_2^{TS}$	−2115.7124756	1.814	2.533		17.3		171.4	139.7	7.6
^{2}**TS2**	^2A	−2115.7637730	1.772	1.513, 1.783	1.650		62.7	131.8	107.2	7.7
^{4}**3**$^+$	$^4A_2$	−2115.7601119	1.877	1.518		127.6		116.2	112.0	10.2
	$^4A_1^{TS}$	−2115.6713208	2.290	1.505		156.8		101.6	166.2	8.2
EC	$^4A_2^{TS}$	−2115.7701289	1.926	3.493		12.3		173.9	103.1	7.7

[a] Signifies H–H bond distance.

3.3.1. $[Ge,C,H_2]^+$

The structural details and relative energetics for all the stationary points located for $[Ge,C,H_2]^+$ are presented in Table 2. In accordance with experimental findings, the cationic global minimum ($^2B_1$) is a ^{2}**1**$^+$ state. According to B3LYP/TZDP, the first excited state is also an electronic isomer of **1**$^+$, the $^2A_1$ state, which lies 36.4 kcal mol^{-1} above the ground state, including zero-point energy (ZPE) corrections. Comparisons of the bond lengths and angles of both isomers clearly show that the excited state can arise from the coupling of ground state CH_2 ($^3B_1$, ∠HCH = 135.3°, r_{CH} = 1.080 Å, B3LYP/TZDP) with Ge^+ (^2P), hence the Ge–C bond order in $^2A_1$ **1**$^+$ is approximately 1.5. On the other hand, coupling of the first methylene excited state ($^1A_1$ CH_2, ∠HCH = 101.5°, r_{CH} = 1.114 Å) with ^2P Ge^+ in a donor–acceptor fashion gives rise to the global minimum. This ion has a much longer Ge–C bond than the first excited state, and is essentially single bonded. The Ge^+–CH_2 interaction in this ion can be rationalised as an a_1 (CH_2) → 4p (Ge^+) donation plus a small amount of 4p (Ge^+) → b_1 (CH_2) back donation that leads to the modest increase in the HCH bond angle. According to our calculations, the global minimum lies 94.8 kcal mol^{-1} below the ^2P Ge^+ + $^3B_1$ CH_2 entrance channel. This value is not much smaller than D(Ge^+–CH) = 107.7 kcal mol^{-1} [3], which possesses a double bond according to our NBO analysis ($^3\Sigma$ $GeCH^+$), so there must be considerable bond strengthening by the back donation in $^2B_1$ $GeCH_2^+$. The lowest energy quartet state of **1**$^+$ ($^4A_2$) is 60.7 kcal mol^{-1} less stable than the ground state.

The classical barrier for the isomerisation of ^{2}**1**$^+$ to

$^2\mathbf{2}^+$ via **TS1** is 51.9 kcal mol^{-1}. The activation energy is calculated to be 48.3 kcal mol^{-1}. This places **TS1** well below the lowest energy exit channels ^2P Ge^+ + $^3B_1$ CH_2 (**TS1** is 46.5 kcal mol^{-1} below) and $^3\Sigma$ $GeCH^+$ + ^2S H (**TS1** is 49.6 kcal mol^{-1} below). Thus, at least in the EI experiments both isomers might be generated. It is doubtful that $^2\mathbf{2}^+$ would be generated if Ge^+ + CH_2 is the only reactant couple, which could be the case in the CI experiments. The classical reverse barrier for the same reaction is calculated to be a mere 2.8 kcal mol^{-1}, and with inclusion of zero-point corrections the activation energy is thus 1.8 kcal mol^{-1}. Given that a significant $^{76}GeH^+$ peak was observed in the CA spectrum of EI-generated $[^{76}Ge,C,H_2]^+$, it can be stated that some of the $\mathbf{2}^+$ observed arises from predissociative isomerisation.

From a theoretical perspective, it is interesting to compare the relative structures of **TS1** for the neutral [13] and cation, and the endothermic reaction products (**2**) on the respective ground state surfaces.

In both the cation and neutral **TS1** structures, the hydrogens are in *trans* configurations. By following the reaction coordinates towards the respective minima, we have verified that the transitions for both the cation and neutral are restricted to planar structures. Moreover, attempts to locate nonplanar $[Ge,C,H_2]^+$ structures of either doublet or quartet spin were largely unsuccessful, with only one high energy nonplanar state $^4\mathbf{1}^+$ (with C_1 symmetry) located (Table 2).

A notable contrast to the neutral and cation **TS1** structures is the much greater Ge–C bond length in the cation, which is clearly a single bond (r_{GeC} = 1.873 Å). We view the depiction of neutral **TS1** in [13] as somewhat misleading, but probably unintentional, because it is clearly a double bond by comparison with experimental bond length values cited by these authors. The H_s–Ge–C bond angle for the cation (this work), where "s" denotes the shifting H atom, is 82.3°, whereas r_{CHs} is 2.295 Å. Both these values are typical for H-shift transition structures.

The hydrogen atoms in the lowest energy isomer of $^2\mathbf{2}^+$ ($^2A''$, this work) are in a *trans* configuration, and this isomer possesses a Ge–C double bond (1.823 Å), in contrast to the corresponding neutral [13], for which this length is significantly shorter (1.727 Å). The Ge–C–H bond angle in the cation and the neutral are almost identical, however, the H–Ge–C bond angle is more acute in the cation. This suggests much greater 4*p* character in σ_{GeH}, as does the somewhat longer cation Ge–H bond (1.546 Å, cf. 1.530 in the neutral), although several of these effects may simply be a reflection of CCSD(T) versus DFT calculations. This point will be addressed shortly.

We also find that linear $^2\mathbf{2}^+$ is a transition structure that is unstable to hydrogen distortions. Thus, the degenerate π frequencies are both imaginary, but it is still a first order saddle point, and the absolute energy difference between linear and *trans* $^2\mathbf{2}^+$ (11.5 kcal mol^{-1}) represents the classical barrier for inversion. According to the highest level calculations of Stogner and Grev, the classical barrier for the analogous neutral reaction is 10.4 kcal mol^{-1}. Both the cation and neutral possess Ge–C triple bonds, and the only distinguishing feature of the $^2\mathbf{2}^+$ structure is a slightly longer C–H bond.

It is worth noting that two *cis* $^2\mathbf{2}^+$ minima were also located in our study, one of which ($^2A'$) closely resembles linear $^2\mathbf{2}^+$ ($^2\Pi$). This particular minimum lies 9.1 kcal mol^{-1} above the linear isomer. In addition, a slight *trans* distortion away from linear $^2\mathbf{2}^+$ yields another minimum, ~1 μhartree higher in energy than linear $^2\mathbf{2}^+$, but with no imaginary frequencies (θ_{HGeC} = 179.0°, θ_{GeCH} = 180.7°). Because of the very flat nature of the doublet potential energy surface (PES) in the vicinity of linear $^2\mathbf{2}^+$, we doubt the existence of this *trans* minimum that may arise from an inadequate quadrature grid density.

The second *cis* minimum ($^2A''$) is 11.4 kcal mol^{-1} more stable than the aforementioned *cis* isomer. This isomer possesses a Ge–C bond of approximate order 2, and the H–Ge–C and Ge–C–H bond angles are more acute (see Table 2). Note that no *cis* isomers were located for the analogous neutral.

For the remainder of the doublet cation surface, no neutral structures have been calculated by Stogner and Grev. The lowest energy $^2\mathbf{3}^+$ minimum on the ground state surface ($^2B_1$) is 106.2 kcal mol^{-1} less stable than the global minimum. If symmetry restrictions on

dissociation are applied, this ion is bound by 37.0 kcal mol^{-1} with respect to the $^2\Pi$ GeC^+ + $^1\Sigma_g$ H_2 exit channel, and by 60.9 kcal mol^{-1} with respect to the $^2A_1$ GeH_2^+ + ^3P C channel. If orbital forbiddeness is ignored, these barriers are lowered by 20.0 kcal mol^{-1} ($^2\Sigma$ GeC^+) and 1.1 kcal mol^{-1} ($^2B_2$ GeH_2^+), respectively. It is important to note that the lowest energy ^{2}**3**$^+$ lies only 9.4 kcal mol^{-1} below the $^1\Sigma$ GeH^+ and $^2\Pi$ CH exit channel. Our search located two valid **TS2** structures, one planar and one nonplanar, which both possess the correct imaginary mode (^2A, 779*i* cm^{-1}, θ_{H_sCGeH} = 102.2°, lying a mere 1.0 kcal mol^{-1} above $^2B_1$ **3**$^+$; and $^2A''$, 489*i* cm^{-1}, lying 4.7 kcal mol^{-1} above $^2B_1$ **3**$^+$). In addition, these structures are nearly isoenergetic, but both lie just above ^{2}**3**$^+$. Given that ^{2}**3**$^+$ is a genuine minimum and is bound with respect to both exit channels, it might be possible to synthesise this isomer from H_2 and GeC^+ in future matrix experiments, but this isomer is likely to be very short lived.

In order to assess the relative quality of our B3LYP/TZDP calculations, the complete singlet neutral surface has been calculated for comparison with the CCSD(T)/DZP, CCSD/TZDP results of Stogner and Grev [13]. Data for the relevant points on the singlet surface are compiled in Table 3. The DFT results are, by far, the best for the ground state geometry. There is, however, a problem with underestimation of the HCH bond angle, but compared with the coupled cluster results of Grev, B3LYP/TZDP would appear to be the method of choice for calculation of an accurate molecular geometry for other alkyl- or alkenyl-germanium species. The lowest energy isomers of **1**/**1**$^+$ and **2**/**2**$^+$ also permit theoretical calculation of the adiabatic ionisation energies of **1** and **2**, which are 8.81 eV and 8.77 eV, respectively. Overall, the B3LYP/TZDP neutral energetics are comparable with those calculated at the relativistically corrected CCSD/TZDP level, with the only difference being a slight underestimation of the reverse barrier for the exothermic ^{1}**2** → ^{1}**1** reaction.

The zero-point energy corrected singlet surface of [Ge,C,H_2] is presented in Fig. 4, together with the doublet surface of the cation. From the results for the singlet surface that we have investigated, it is evident there is little prospect of synthesising either neutral **2** or **3**, as both species reside in very shallow minima and isomerisation should be facile in both cases. This is also the situation for the cation, for which generation of **2**$^+$ and **3**$^+$ will require high temperatures. The propensity for the excited neutrals, formed by vertical recombination, to overcome isomerisation barriers can be derived from a set of single point calculations and the optimised neutral structures. For example, vertical recombination imparts 13.8 kcal mol^{-1} to the neutral ^{1}**1**, whereas 12.0 kcal mol^{-1} internal energy is imparted to the neutral ^{1}**2**. Any hyperthermal ^{1}**2** would thus undergo isomerisation to ^{1}**1** because 13.1 kcal mol^{-1} suffices for this activation.

We now turn our attention to the quartet surface of the cation. As discussed previously, the lowest energy isomer on this surface is ^{4}**1**$^+$ ($^4A_2$), which lies 60.7 kcal mol^{-1} above the global minimum, but is still bound by 34.1 kcal mol^{-1} and 32.9 kcal mol^{-1} with respect to the lowest energy $^2Ge^+$ + $^3CH_2$ and $^3GeCH^+$ + ^2H channels. We can unequivocally state that the unimolecular ^{4}**1**$^+$ ⇄ ^{4}**2**$^+$ interconversion is not feasible because the ^{4}**TS1** for this reaction lies well above both of the aforementioned spin-allowed dissociation asymptotes. Concerning the quartet minimum ^{4}**2**$^+$, the H atoms are in a *cis* configuration, and this isomer lies 65.9 kcal mol^{-1} above the global minimum. The Ge–C bond length in this isomer is consistent with a contracted single bond, and geometrically the structure of this ion is similar to the lowest energy *cis* ^{2}**2**$^+$ ($^2A''$). Two linear and one *trans* ^{4}**2**$^+$ stationary points were also located, but all were saddle points lying well above the lowest energy $^3GeCH^+$ + ^2H channel. One of these ($^4\Sigma$) represents an encounter complex for $^3\Sigma$ $GeCH^+$ and ^2S H, if indeed it is a genuine stationary point and not an artefact of the exchange-correlation grid.

The lowest energy isomer of ^{4}**3**$^+$ ($^4A_2$) is bound by 25.1 kcal mol^{-1}, 53.9 kcal mol^{-1}, and 55.1 kcal mol^{-1} with respect to the lowest spin-allowed $^1GeH^+$ + ^4CH, $^2GeH_2^+$ + ^3C, $^3HGeC^+$ + ^2H asymptotes, but is unbound by 15.7 kcal mol^{-1} with respect to the lowest energy $^4GeC^+$ + $^1H_2$ asymptote. Exit via the last pathway is formally orbital forbidden and will be associated with a barrier corre-

Table 3
Theoretical results for selected stationary points on the singlet surface of [Ge,C,H_2]. Relative energies (ZPE corrected) are in units of kcal mol^{-1}, bond lengths are in Å, angles are in degrees, and vibrational frequencies in cm^{-1}. "TS" signifies a saddle point

	Parameter	B3LYP/TZDP	CCSD(T)/DZP[a]	CCSD/TZDP[a]
$^1A_1$ $GeCH_2$[b]	E_{rel}	0.0	0.0	0.0
	r_{GeC}	1.800	1.823	1.805
	r_{CH}	1.102	1.097	1.086
	θ_{HCH}	113.8	113.7	114.1
	$\nu_1(a_1)$	3082	3122	3128
	$\nu_2(a_1)$	1341	1372	1369
	$\nu_3(a_1)$	784	760	795
	$\nu_4(b_1)$	685	648	683
	$\nu_5(b_2)$	3165	3219	3217
	$\nu_6(b_2)$	407	396	404
$^1A'$HGeCH	E_{rel}	47.4	45.0	49.5
	r_{GeC}	1.720	1.753	1.727
	r_{CH}	1.082	1.090	1.077
	r_{GeH}	1.533	1.532	1.530
	θ_{GeCH}	147.9	143.4	145.2
	θ_{HGeC}	122.7	126.0	127.9
	$\nu_1(a')$	307	441	394
	$\nu_2(a'')$	526	549	563
	$\nu_3(a')$	780	721	738
	$\nu_4(a')$	939	894	950
	$\nu_5(a')$	2098	2172	2174
	$\nu_6(a')$	3249	3271	3294
$^1\Sigma^+$HGeCH[TS]	E_{rel}	56.5	57.1	58.7
	r_{GeC}	1.643	1.676	1.658
	r_{CH}	1.070	1.078	1.067
	r_{GeH}	1.484	1.496	1.494
$^1A'$HGeCH[TS]	E_{rel}	48.8	52.0	54.3
	r_{GeC}	1.762	1.781	1.772
	r_{CH}	1.085	1.093	1.080
	r_{GeH}	1.581	1.596	1.588
	θ_{GeCH}	168.2	171.1	170.3
	θ_{HGeC}	86.8	79.9	83.4

[a] Coupled cluster results from [13].
[b] Experimental values are: r_{GeC} = 1.790 Å, r_{CH} = 1.102 Å, θ_{HCH} = 115.1. From [12].

lating with a Rydberg state of $^4GeC^+$. Judging by the relative energies of these asymptotes, it appears that conversion between $^4\mathbf{2}^+$ and $^4\mathbf{3}^+$ might be feasible on the excited surface, even if it is energy demanding and ions produced with three unpaired electrons are short-lived with respect to spin inversion. Analysis of the normal mode corresponding to the lowest frequency of $^4\mathbf{3}^+$ reveals it has out-of-plane bending character (b_1), consistent with dissociation via the $^4GeC^+ + {}^1H_2$ asymptote, so we have instead chosen to follow the next lowest vibrational mode uphill, corresponding to the GeH_2 rocking motion (b_2). Eventually, this led to a first-order saddle point with a rather low imaginary frequency of $80i$ cm^{-1} [$^4A''$, $r_{Ge\text{-}C}$ = 2.292 Å, $r_{Ge\text{-}H_s}$ = 1.670 Å, $r_{Ge\text{-}H}$ = 1.736 Å, θ_{CGeH_s} = 64.7°, θ_{HGeH_s} = 158.6°, E(B3LYP/TZDP) = −2115.6926705 hartrees]. This structure closely resembles the endothermic reaction product $^4\mathbf{3}^+$, in accordance with Hammond's postulate [28]. However, further displacement of this structure toward $^4\mathbf{2}^+$ generated a saddle point with two imaginary frequencies. Given that approaching $^4\mathbf{2}^+$ from the lowest energy quartet $^4\mathbf{3}^+$ isomer was unsuccessful, we also attempted to locate a first-order saddle point

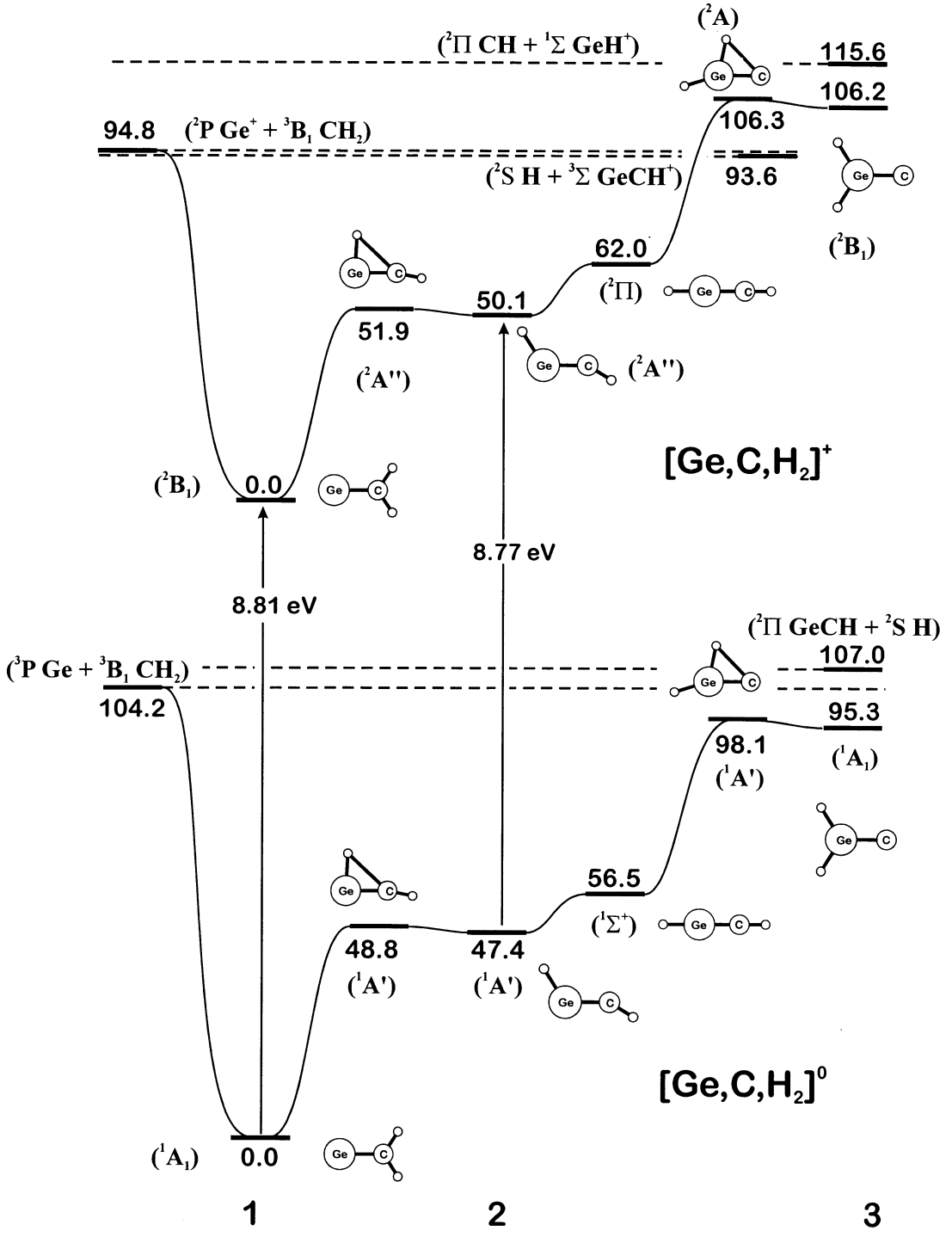

Fig. 4. Singlet potential-energy surface of neutral [Ge,C,H_2] (bottom), and doublet potential-energy surface of [Ge,C,H_2]$^+$ derived from B3LYP/6-311++G(d,p). The singlet surface of the neutral has also been calculated using CCSD(T)/TZDP (see [13]). The numbers at the base of the diagram are given according to Scheme 1.

Table 4
Results for selected stationary points on the $[Ge,C,H_3]^+$ singlet and triplet surfaces located using B3LYP/6-311++G(d,p). SCF energies are in hartrees, bond lengths in Å, zero-point and E_{rel} (ZPE corrected) energies in kcal mol^{-1}. "TS" signifies a saddle point

Structure	State	E_{SCF}	r_{GeC}	r_{GeH}	r_{CH}	$\theta_{HCH°}$	$\theta_{GeCH°}$	$\theta_{HGeC°}$	E_{rel}	ZPE
Cations										
^{1}**4**$^+$	$^1A_1$	−2116.6055964	1.918		1.100	107.7	111.2		0.0	21.2
^{3}**4**$^+$	^3A	−2116.5273279	2.226		1.092	116.0	97.7		48.9	20.6
					1.087, 1.088	116.2	101.6			
						118.0	102.1			
^{1}**5**$^+$	$^1A'$	−2116.5241147	1.818	1.533	1.093	106.7	119.3	124.5[a]	48.6	18.6
	$^1A_1^{TS}$	−2116.5164511	1.733	1.506	1.087	120.8	119.6	180.0	53.3	18.1
	$^1A'^{TS}$	−2116.5202952	1.895	1.583	1.095	112.4	123.3	85.2[b]	50.4	17.6
^{3}**5**$^+$	$^3A''$	−2116.5075648	1.898	1.549	1.090, 1.086	118.2	119.7	118.3	59.4	18.6
							122.1			
	$^3A_2^{TS}$	−2116.4654529	1.872	1.503	1.086	121.2	119.4	180.0	85.4	17.9
	$^3A^{TS}$	−2116.4461184	2.159	1.623	1.083, 1.092	132.9	103.3	67.8[c]	95.5	15.8
							118.2			
Neutrals										
CH_3	$^2A''_2$	−39.8551874			1.080	120.0				18.6
^{2}**4**	$^2A''$	−2116.86300	2.003		1.100, 1.094, 1.094		106.4,		0.0	21.2
							113.2			
^{2}**4**[d,e]	$^2A'$	−2116.86289	2.004		1.093, 1.097, 1.097		109.4,		0.0	20.6
							114.2			
^{4}**4**	$^4A''$	−2116.80349	2.226		1.084		101.9		68.0[f]	
^{4}**4**[d]	$^4A''$	−2116.75557	2.129		1.086		104.1		44.7	21.1

[a] θ_{H_aGeCH} = 106.7°.
[b] θ_{H_aGeCH} = 96.4°.
[c] θ_{H_aGeCH} = 52.0°, 28.8°.
[d] Results from B3PW91/6-311G* calculations are: $^2A'$ (ground state), E_{SCF} = −2116.82621 hartrees, r_{GeC} = 1.999 Å, r_{CH} = 1.101 Å, 1.094 Å, 1.094 Å, θ_{GeCH} = 106.0°, 113.6°, ZPE = 21.2 kcal mol^{-1}, from [29].
[e] $^2A''$ is the ground state according to B3LYP/TZDP calculations. $^2A'$ is a transition structure possessing an imaginary frequency, 544*i* cm^{-1}.
[f] SCF energy difference (no ZPE correction).

starting from the *cis* ^{4}**2**$^+$ isomer. Again, this was done by following the lowest vibrational frequency corresponding to the desired H-shifting motion, uphill. During this study, the bond lengths of the model TS were kept fixed and the H–Ge–C and Ge–C–H_s bond angles varied. In the highest energy first-order saddle point that was located [$^4A''$, ω = 792*i* cm^{-1}, $r_{Ge\text{-}C}$ = 1.89 Å, $r_{C\text{-}H_s}$ = 1.52 Å, $r_{Ge\text{-}H}$ = 1.56 Å, E(B3LYP/TZDP) = 2115.72615326 hartrees], these bond angles were 110° and 75°, respectively. Inspection of the imaginary mode of this structure revealed large amplitude motions for both H atoms *away* from the GeC^+ moiety, thus corresponding to a dihydrogen elimination reaction path. Thus, we conclude that ^{4}**3**$^+$ ⇄ ^{4}**2**$^+$ is impossible, but do not preclude the synthesis of ^{4}**3**$^+$ from the appropriate reactant couples.

3.3.2. [Ge,C,H$_3$]$^+$

To the best of our knowledge, there is no information available for $[Ge,C,H_3]^+$, and only one previously published study of the neutral **4** [29]. B3PW91/TZP geometric parameters, obtained in this work for the lowest energy doublet and quartet isomers of $GeCH_3$ are presented in Table 4, together with the B3LYP/TZDP results for singlet and triplet $\mathbf{4}^+$ and $\mathbf{5}^+$. The singlet and triplet surfaces in the vicinity of these isomers is also presented in Fig. 5.

In accordance with the experimental results, the global minimum on the $[Ge,C,H_3]^+$ surface is predicted to be $^1\mathbf{4}^+$. This ion is bound by 78.6 kcal mol^{-1} and 94.2 kcal mol^{-1} with respect to the $^2Ge^+$ + $^2CH_3$ ($^2A''_2$) and $^2GeCH_2^+$ ($^2B_1$) + ^2H asymptotes. The global minimum has high symmetry (C_{3v}), consistent

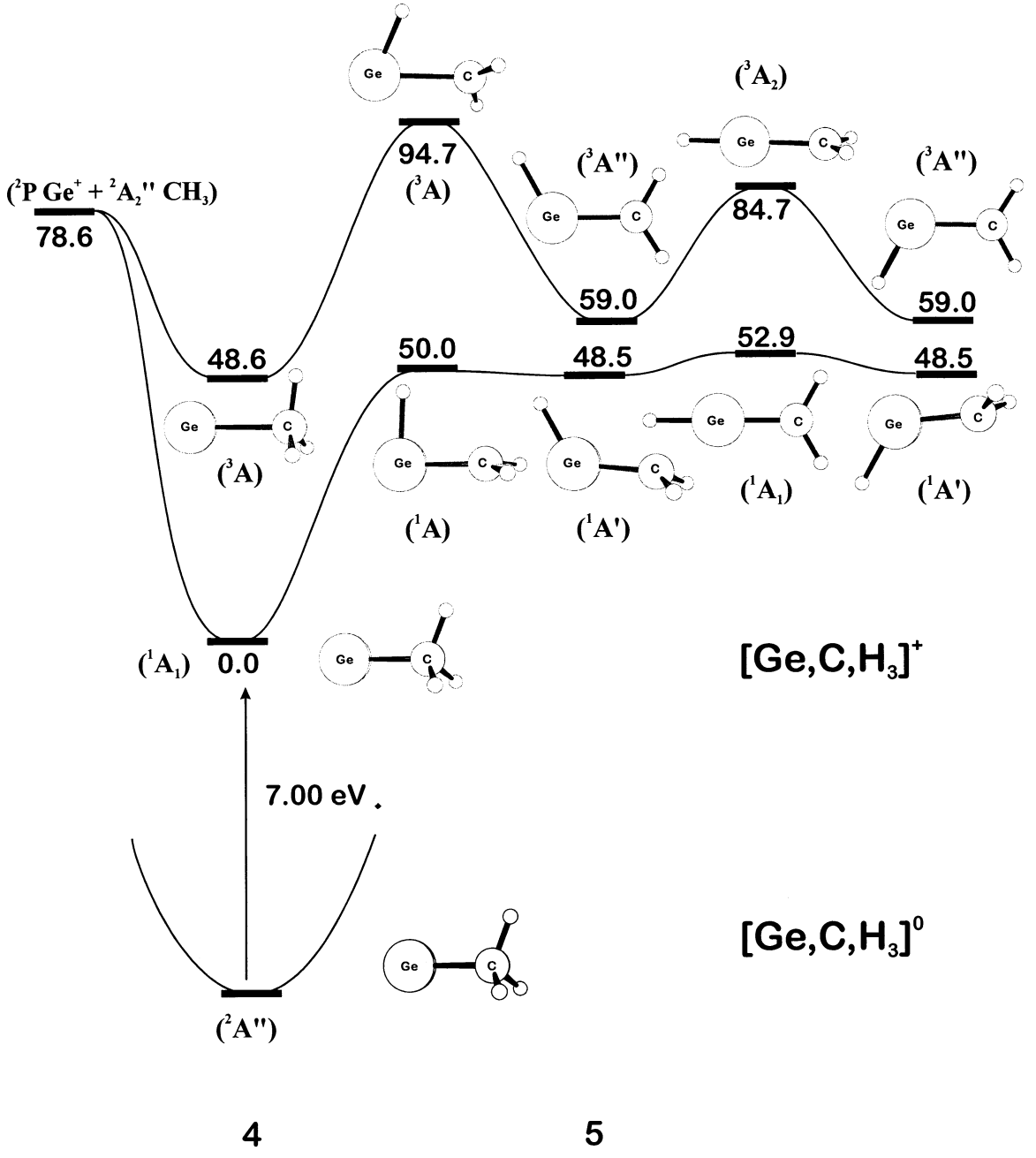

Fig. 5. Singlet and triplet potential-energy surfaces for the interconversion of $GeCH_3^+$ and $HGeCH_2^+$ as derived from B3LYP/6-311++G(d,p) calculations. The numbers at the base of the diagram are given according to Scheme 1.

with coupling of the unpaired 4*p* electron of ^2P Ge^+ with the unpaired a''_2 electron of CH_3 to yield a closed shell ion. The Ge–C bond length (1.918 Å) is rather short and can be attributed to Coulombic attraction between the positively charged Ge and the electron-rich C atom. C–H bond elongation in $^1\mathbf{4}^+$ with respect

to free ($^2A''_2$) CH_3 is the result of resonance interactions between the nonbonding $4s^2$ Ge electrons and the σ^*_{CH} orbitals.

The transition structure for the conversion of $^1\mathbf{4}^+$ to $^1\mathbf{5}^+$ lies 50.0 kcal mol^{-1} above the global minimum. This is well below the energies required for loss of H and CH_3, so a mixture of isomers could be generated in the MS experiments. Given that $^1\mathbf{5}^+$ resides in a very shallow potential minimum, and the magnitude of the reverse activation barrier (1.5 kcal mol^{-1}), it is doubtful whether the yields of $^2\mathbf{5}^+$ would be sufficient for its spectroscopic detection.

Relative to the global minimum, $^1\mathbf{5}^+$ represents the lowest energy isomer (structural or electronic) that was located in our potential-energy searches. The Ge–C bond in $^1\mathbf{5}^+$ has approximate order 1.5–2, and the distinctive feature of its structure is that it is three-dimensional, with the methylene hydrogens positioned *trans* with respect to the hydrogen attached to Ge^+. The origin of the bending can be traced to repulsions between the nonbonding electron residing on Ge^+ (sp character) and the unpaired methylene electron. Investigations of the C_{2v} analogue of this structure (flat with linear H–Ge–C connectivity) established that this configuration is a transition structure for inversion of the *trans* isomer, and requires a mere 4.4 kcal mol^{-1} according to B3LYP/TZDP. Thus, we conclude that the prospects of generating useful yields of $\mathbf{5}^+$ or $\mathbf{6}^+$ on the ground state (singlet) PES are not good, and turn our attention to the excited surface.

The lowest energy triplet ($^3\mathbf{4}^+$) lies 48.6 kcal mol^{-1} above the global minimum. The computed structure is entirely asymmetric (^3A), which is attributed to both a flat PES and grid deficiencies. The Ge–C bond length in this isomer (2.226 Å) is very long, and suggests the ion–dipole interaction is predominantly responsible for stabilisation. This species arises from a a''_2 (CH_3) $\rightarrow$ 4*p* (Ge) donation with some back donation from Ge 4*p* to the in-plane σ^*_{CH} orbital. An elongated C–H bond (1.092 Å, cf. 1.087 Å and 1.088 Å) with a significantly smaller Ge–C–H bond angle, is a manifestation of this effect. The Ge^+-CH_3 binding energy is calculated to be 29.7 kcal mol^{-1} with respect to ^2P Ge^+ + $^2A''_2$ CH_3. ^{3}**TS1** for the conversion $^3\mathbf{4}^+ \rightarrow {}^3\mathbf{5}^+$ lies 94.7 kcal mol^{-1} above the global minimum, so this reaction is not feasible because it is well above the asymptote for Ge^+–CH_3 bond dissociation. In marked contrast to the singlet surface, $^3\mathbf{5}^+$ resides in a reasonably deep potential minimum, with the reverse activation barrier being 35.7 kcal mol^{-1}, and dissociation via $^1GeH^+$ + $^3CH_2$ requiring 50.0 kcal mol^{-1}. It is a mere 10.4 kcal mol^{-1} less stable than the analogous singlet isomer. The structure of $^3\mathbf{5}^+$ closely resembles the structure of vinyl cation ($C_2H_3^+$), that is, it is planar, and all of the bond angles are close to 120°. Naturally, the transition structure connecting three-dimensional $^3\mathbf{5}^+$ with planar $^3\mathbf{4}^+$ is also three-dimensional, but more closely resembles the latter than the former because the dihedral angle between the gauche hydrogens is 52.0°. Finally, the fact that reversion to $^3\mathbf{4}^+$ from $^3\mathbf{5}^+$ is not feasible, suggests there might be some chance of observing $^3\mathbf{5}^+$, however, this will require electronic excitation. Moreover, the lifetime of the high spin ions formed may only be short, due to non-negligible spin-orbit coupling for Ge, hence detection of this interesting ion and its corresponding neutral represents a significant challenge.

4. Conclusions

CA experiments have established that the species $[Ge,C,H_n]^+$, n = 2–3, generated by CI of GeH_4/*c*-C_3H_6 mixtures and EI of Cl_3GeCH_3 vapour, possess predominantly, if not exclusively, Ge^+-CH_n connectivities. All of the ions $GeCH_n^+$ yield recovery signals in $^+NR^+$ experiments. As far as isomers containing Ge–H bonds are concerned, theoretical studies have revealed that these isomers will only be detected at elevated temperatures (for instance, after annealing in matrix experiments), and then only in small amounts. In particular, the ground state surfaces of the cations and neutrals we have investigated are characterised by small, and sometimes insignificant, barriers separating $GeCH_n \rightarrow HGeCH_{n-1}$ ($n < 3$). Given the finite possibility of predissociative isomerisation, it is unclear whether isomers with $HGeCH_{n-1}^+$, $n < 3$, are formed in the ion source or by collisional activation

events. The NR results have confirmed the existence of $GeCH_3$, and together with the CA results, provide the first experimental structural evidence that both the ion and neutral possess predominantly methylgermanium connectivity.

Acknowledgements

This research was supported by the Deutsche Forschungsgemeinschaft, the Volkswagen-Stiftung, and the Fonds der Chemischen Industrie. The Konrad-Zuse Zentrum, Berlin, is acknowledged for generous allocation of computer time. We would like to thank Dr. S.J. Blanksby for help with the literature review, and Professor Y. Apeloig for many helpful discussions. RS gratefully acknowledges support from the DAAD (visiting fellowship) and the guidance of Dr. K.V. Raghavan, Director, Indian Institute of Chemical Technology.

References

[1] S.G. Lias, J.F. Liebman, R.D. Levin, S.A. Kafafi, NIST Standard Reference Database 19A, Version 2.01, National Institute of Standards and Technology, Gaithersburg, MD, 1994.
[2] M. Karni, Y. Apeloig, D. Schröder, W. Zummack, R. Rabenazza, H. Schwarz, Angew. Chem. Int. Ed. Engl. 38 (1999) 332.
[3] P. Jackson, M. Diefenbach, D. Schröder, H. Schwarz, Eur. J. Inorg. Chem. (1999) 1203.
[4] M.R. Hoffmann, Y. Yoshioka, H.F. Schaefer, III, J. Am. Chem. Soc. 105 (1983) 1084.
[5] A.C. Hopkinson, M.H. Lien, Chem. Commun. (1980) 107.
[6] R. Stegman, G. Frenking, J. Comput. Chem. 17 (1996) 781.
[7] R. Srinivas, D. Sülzle, H. Schwarz, J. Am. Chem. Soc. 113 (1991) 52.
[8] B.T. Luke, J.A. Pople, M-B. Krogh-Jespersen, Y. Apeloig, M. Karni, J. Chandrasekhar, P. von Rague-Schleyer, J. Am. Chem. Soc. 108 (1986) 270.
[9] K.P. Lim, F.W. Lampe, Int. J. Mass Spectrom. Ion Processes 101 (1990) 245.
[10] R. Srinivas, P. Jackson, S.J. Blanksby, H. Schwarz, unpublished results.
[11] P. Jackson, R. Srinivas, S.J. Blanksby, D. Schröder, H. Schwarz, unpublished.
[12] D.A. Hostutler, T.C. Smith, H. Li, D.J. Clouthier, J. Chem. Phys. 111 (1999) 950.
[13] S.M. Stogner, R. Grev, J. Chem. Phys. 108 (1998) 5458.
[14] A.D. Becke, Phys. Rev. A 38 (1988) 3088.
[15] A.D. Becke, J. Chem. Phys. 98 (1993) 5648.
[16] For the most recent review of the NRMS technique, see: C.A. Schalley, G. Hornung, D. Schröder, H. Schwarz, Chem. Soc. Rev. 27 (1998) 91. See also references cited therein.
[17] P. Jackson, K.J. Fisher, I.G. Dance, G.E. Gadd, G.D. Willett, Int. J. Mass Spectrom. Ion Processes 164 (1997) 45.
[18] L. Operti, M. Splendore, G.A. Vaglio, P. Volpe, M. Speranza, G. Occhiucci, J. Organomet. Chem. 433 (1992) 35.
[19] M. Castiglioni, L. Operti, R. Rabezzana, G.A. Vaglio, P. Volpe, Int. J. Mass Spectrom. 179/180 (1998) 277.
[20] P. Antoniotti, P. Benzi, M. Castiglioni, P. Volpe, Eur. J. Inorg. Chem. (1999) 323.
[21] J.L. Holmes, Org. Mass Spectrom. 20 (1985) 169.
[22] K.L. Busch, G.L. Glish, S.L. McLuckey, Mass Spectrometry/Mass Spectrometry: Techniques and Applications of Mass Spectrometry, VCH, Weinheim, 1988.
[23] M.J. Frisch, G.W. Trucks, H.B. Schlegel, P.M.W. Gill, B.G. Johnson, M.A. Robb, J.R. Cheeseman, T.A. Keith, G.A. Petersson, J.A. Montgomery, K. Raghavachari, M.A. Al-Laham, V.G. Zakrzewski, J.V. Ortiz, J.B. Foresman, J. Cioslowski, B.B. Stefanov, N. Nanayakkara, M. Challacombe, C.Y. Peng, P.Y. Ayala, W. Chen, M.W. Wong, J.L. Andres, E.S. Replogle, R. Gomperts, R.L. Martin, D.J. Fox, J.S. Binkley, D.J. DeFrees, J. Baker, J.P. Stewart, M. Head-Gordon, C. Gonzales, J.A. Pople, GUASSIAN 94, Gaussian Inc., Pittsburgh, PA, 1995.
[24] R. Krishnan, J.S. Binkley, R. Seeger, J.A. Pople, J. Chem. Phys. 72 (1980) 650.
[25] R.C. Binning, L.A. Curtiss, J. Comp. Chem. 11 (1990) 1206.
[26] L.A. Curtiss, M.P. McGrath, J.-P. Blandeau, N.E. Davis, R.C. Binning, L. Radom, J. Chem. Phys. 103 (1995) 6104.
[27] M.P. McGrath, L. Radom, J. Chem. Phys. 94 (1991) 511.
[28] G.S. Hammond, J. Am. Chem. Soc. 77 (1955) 334.
[29] J.L. Belbruno, J. Chem. Soc. Faraday Trans. 94 (1998) 1555.